A simplified approach for flood modeling in urban environments

Xushu Wu, Zhaoli Wang, Shenglian Guo, Chengguang Lai
and Xiaohong Chen

ABSTRACT

A rapid increase in the risk of urban flooding in recent years has urged the research community to enrich approaches to deal with urban flooding problems. The state-of-the-art approach consists of coupling one-dimensional (1D) and two-dimensional (2D) hydrodynamic models. However, at present such coupled 1D/2D models are mostly commercial and complex to build and run. The present study has proposed a new simple approach for modeling urban flooding by coupling Storm Water Management Model (SWMM) and LISFLOOD-FP, two widely used freewares with relatively simple components. The coupled model was firstly applied to the Shiqiao Creek District in Dongguan City, South China, and verified against four major historical floods. The testing results demonstrate the capability of the coupled model in predicting urban flooding. The successful coupling of SWMM and LISFLOOD-FP offers another simple, practical approach for urban flooding estimation, which can be readily used by non-expert users or those who do not have access to commercial modules.

Key words | coupling approach, LISFLOOD-FP, SWMM, urban flooding

Xushu Wu
Shenglian Guo
State Key Laboratory of Water Resources and
  Hydropower Engineering Science,
Wuhan University,
Wuhan 430072, China

Xushu Wu
Zhaoli Wang (corresponding author)
Chengguang Lai
School of Civil Engineering and Transportation,
South China University of Technology,
Guangzhou 510640, China
E-mail: wangzhl@scut.edu.cn

Zhaoli Wang
Chengguang Lai
State Key Laboratory of Subtropical Building
  Science,
South China University of Technology,
Guangzhou 510640, China

Xiaohong Chen
Center for Water Resources and Environment
  Research,
Sun Yat-sen University,
Guangzhou 510275, China

INTRODUCTION

Flooding in urban areas is characterized by strong intensity and a short response time that would cause enormous human and economic losses (Apel *et al.* 2009). With changes in global climate and urbanization, urban flood is increasing and resultant damage has been reported worldwide (Lin *et al.* 2014). As a consequence, it still remains a challenging issue for hydrologists and needs further investigation (Kjeldsen *et al.* 2013; Paz *et al.* 2016).

Flood dynamics across urbanized areas are difficult to understand because of the complex urban infrastructures, underlying surface conditions and drainage systems, which play important roles in flood propagation and accumulation (Leandro *et al.* 2016). Scientists have sought to study urban

flood by means of different methodologies, including investigation of historical floods (Swan 2010), indicator-based flood assessment (Leitão *et al.* 2013), and numerical modeling (Liang & Smith 2015). Among these, numerical modeling is an effective and prevailing method to deal with urban flood problems at present (Leandro *et al.* 2009; Bach *et al.* 2014). Considerable progress has been made in the development and application of hydrologic/hydraulic models for urban flood simulation over the past decades. The typical models that are broadly recognized include the MIKE 21, XP-SWMM (XP Software 2013), InfoWorks RS (Salarpour *et al.* 2011), and so on. These models respectively use one-dimensional (1D) sewer models and

two-dimensional (2D) overland models for flow routings along the pipelines and the ground surfaces covered with buildings, streets and sidewalls, and are capable of reproducing the interaction between sewer systems and overland surfaces (Seyoum *et al.* 2012; Willems *et al.* 2012). While these models are proved able to make reasonable predictions of the likely flood damage, their abilities can vary with the objective of the study, the characteristics of the study region, and data availability (Bach *et al.* 2014; Chang *et al.* 2015). It is therefore impossible to identify a universal model which is best suitable for modeling urban flood. On the other hand, the foregoing models are mostly commercial and non-open for users, which, to some extent, has hampered their widespread use. Indeed this would become a major problem for researchers or engineers who do not have access to commercial modules, due to lack of model techniques for the study of urban flood processes.

Limited attempts have been made to propose other approaches for urban flooding estimation without access to commercial modules so far. Some researchers have coupled pre-existing open-source 1D sewer models with 2D overland models (e.g. Leandro *et al.* 2009; Paz *et al.* 2016), while others have developed their own 1D (2D) models and integrated them with existing 2D (1D) models (e.g. Seyoum *et al.* 2012). The former approach is much more simplified and commonly used than the latter one, largely because it does not rely heavily on specialized programing knowledge. Generally, for coupling existing 1D and 2D models, researchers usually employ the open-source Storm Water Management Model (SWMM), known as a simple but robust 1D sewer model, to calculate hydraulics in pipelines (Leandro & Martins 2016). However, there is little agreement on the choice of 2D overland models. More recently, with the increasing availability of high resolution Digital Elevation Models (DEMs) and extensive use of Geographic Information System (GIS), raster-based 2D hydrodynamic models are preferable because they can be readily integrated with DEMs, simplifying model setup and post-processing (Paz *et al.* 2016). LISFLOOD-FP, first developed by Bates & De Roo (2000), is a raster-based 2D model that has been well demonstrated to be able to predict flood inundation (Bates *et al.* 2010). With relatively simple formulation, LISFLOOD-FP is easy to set up and run, computationally

efficient, and suitable for non-expert users. Inspired by this, the authors firstly coupled SWMM and LISFLOOD-FP in the present research, with the aim to provide another alternative for urban flood modeling.

In the coupling 1D/2D model framework, estimation of the interacting discharge between sewer and overland models is fairly important because it has a significant impact on model performance. Previous studies have adopted weir and orifice formulas to calculate the interacting discharge (Seyoum *et al.* 2012; Chen *et al.* 2015). These formulas make an assumption of the completely open state of manholes (i.e. without covers). In the real-world, however, manholes are usually covered and their discharge capacities may be much lower than expected. In this regard, the interacting discharge may be overestimated if manholes are regarded as completely open, which could result in a large deviation in model results. Even if a model is tested to perform well in an application without consideration to the manhole cover effect, the parameter specification might be 'unreal' and suspicious resulting from the equifinality effect (Her & Chaubey 2015). To reveal the role of the manhole cover in modeling, in this paper the authors preliminarily discuss its effect on parameter specification and model performance in some example applications.

The paper is organized as follows: the next section describes SWMM and LISFLOOD-FP model structures and the method to couple them. Then example applications of the coupled model and the testing results are presented. Next, a brief discussion is given and finally, the conclusion is presented.

MODEL DESCRIPTION AND METHODOLOGY

SWMM and LISFLOOD-FP

Introduced in 1971, SWMM is considered a landmark of urban hydrologic models and is broadly regarded as an efficient 1D sewer model (Delleur 2003). It is capable of simulating runoff quantity and quality according to the 1D Saint-Venant equations from primarily urban areas. In the SWMM framework, the whole study area is divided into a collection of sub-catchments that receive precipitation and

generate runoff. The surface runoff in a sub-catchment flows entirely into a single outlet (manhole or any other sub-catchment) and thus there is no surface routing in SWMM. Storm water is then transported in pipes, channels, storage/treatment devices, pumps, and regulators, and finally flows toward the area outlets. In SWMM, when all pipes connected to a manhole are full of storm water, or when the water surface at the manhole is between the crown of the connected highest pipe and the ground surface, surcharging will occur. Flooding takes place when the hydraulic grade line is above the ground surface. A detailed description of SWMM can be found in earlier studies (Delleur 2003; Leandro & Martins 2016). There have been several versions of SWMM since its first release and this study employed the latest version (SWMM5) which was downloaded from https://www.epa.gov/water-research/storm-water-management-model-swmm#downloads.

LISFLOOD-FP is a raster-based hydraulic model originally developed by Bates & De Roo (2000). It can reflect the flood process and yield good prediction of maximum flood extent (Bates *et al.* 2010). An intelligent volume-filling process based on hydraulic principles and the key physical notions of mass conservation and hydraulic connectivity, are both used in the model, to treat flooding (Bates *et al.* 2010). Like SWMM, this model has been improved since its first release, and in the study the freeware of LISFLOOD-FP (V5.9.6) which was recently released was used. It is available under http://www.bristol.ac.uk/geography/research/hydrology/models/lisflood/downloads/. The basic formulations of LISFLOOD-FP (V5.9.6) are described in detail in some existing publications (Bates *et al.* 2010; de Almeida *et al.* 2012).

SWMM and LISFLOOD-FP linkage

SWMM and LISFLOOD-FP are combined for simulating the flow dynamics in sewers and on overland surfaces. The hydrological rainfall-runoff process and flow routing in pipelines are performed through SWMM, while surcharged flows that spill onto the ground surface from manholes are routed on the 2D domain by using LISFLOOD-FP. For floodplains with river networks, LISFLOOD-FP is applied to solve 2D floodplain flows and 1D river flows.

The models are linked by exchanging information at the connecting nodes (manholes) and the 2D grids containing the manholes are regarded as the locations where the interactions occur. Given that the coupled model employs LISFLOOD-FP freeware without access to the source code (currently unavailable), the two models are executed separately and repeatedly during a complete simulation. In other words, for each execution, both models run within a small, equivalent time interval (see the timing synchronization section) and at the end of the execution the initial conditions (see the interacting discharge section) of SWMM and LISFLOOD-FP are updated for the next execution. A program is compiled on a C# platform to invoke SWMM and LISFLOOD-FP engines and force both models to exchange information during each execution process.

Timing synchronization

The time step of SWMM is fixed and can be reset before execution, however that of LISFLOOD-FP is variable and determined by the model itself and thus cannot be changed manually (Bates *et al.* 2010). Therefore, for each execution either the SWMM time step or the execution time of LISFLOOD-FP should be adjusted to ensure that the two models run within the same time interval and exchange information properly.

Let Δt_{i_swmm}, $\Delta t_{i\_lisflood}$ and $t_{i\_lisflood}$ be the SWMM and LISFLOOD-FP time steps and the execution time of LISFLOOD-FP for the *i*th execution, respectively. In the case that $\Delta t_{i\_swmm} \geq \Delta t_{i\_lisflood}$, $t_{i\_lisflood}$ is adjusted as:

$$t'_{i\_lisflood} = \Delta t_{i\_swmm} \tag{1}$$

In Equation (1), Δt_{i_swmm} is also considered as the *i*th execution time of SWMM.

In the case that $\Delta t_{i\_swmm} < \Delta t_{i\_lisflood}$, the magnitude of Δt_{i_swmm} is adjusted as:

$$\Delta t'_{i\_swmm} = \Delta t_{i\_lisflood} \tag{2}$$

In Equation (2), $\Delta t_{i\_lisflood}$ is also considered as the *i*th execution time of LISFLOOD-FP. Equations (1) and (2)

indicate that for the ith execution, the simulation times of the two models are equivalent, enabling the two models to exchange information at the same time (Figure 1).

Interacting discharge

In the coupled model scheme, the overflows/inflows from sewers/ground to ground/sewers through manholes at the end of each execution are treated as point sources (i.e. initial conditions) of LISFLOOD-FP/SWMM for the next execution. As stated in the introduction section, the effect of a manhole-cover on such interacting discharge should not be neglected. Given that there is no theoretical or empirical formula available to measure the effect of a manhole-cover on interacting discharge, this paper introduces a reduction coefficient to preliminarily reflect such an effect, and accordingly modifies the previous proposed weir and orifice formulas to compute interacting discharge. To the best of the authors' knowledge, the reduction coefficient is largely determined by the shape of the manhole-cover, which can be estimated through the following equation:

$$\lambda = \frac{A}{A_0} \tag{3}$$

in which A and A_0 represent the flow cross-sectional area and geometric cross-sectional area of the manhole, respectively.
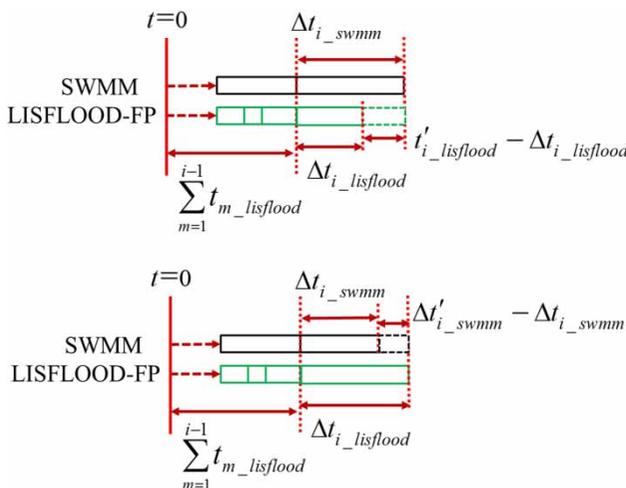
Figure 1 | Timing synchronization between SWMM and LISFLOOD-FP.

According to Chen *et al.* (2015), the interacting discharge should be calculated by the water level difference between the sewer network and the above-ground surface. Let h_U and h_D be the upstream and downstream water levels, which are defined as:

$$h_U = \max\{h_m, h_d\} \tag{4}$$

$$h_D = \min\{h_m, h_d\} \tag{5}$$

where h_m and h_d are the hydraulic head at the manhole and the water surface elevation on the 2D overland grid, respectively. The crest elevation of a manhole may differ from the ground elevation of the overland grid containing the manhole, therefore, to avoid inaccuracies that result from inconsistency between two data sets, the crest elevation, z_{crest} is determined by:

$$z_{crest} = \max\{z_m, z_d\} \tag{6}$$

where z_m and z_d are the crest elevation of the manhole and 2D grid elevation, respectively.

In the case that $h_D < z_{crest} < h_U$, the discharge is calculated based on the free weir formula and the reduction coefficient:

$$Q = sign\{\lambda[h_m - h_d]cW\sqrt{2g}(h_U - z_{crest})^{3/2}\} \tag{7}$$

where c is the weir discharge coefficient and W is the weir crest width. λ is the reduction coefficient described above. Positive/negative Q indicates surcharge/drainage flow from sewer/overland to overland/sewer.

In the case of $z_{crest} < h_D < h_U$ and $h_U - z_{crest} < (A_0/W)$, the submerged weir formula is adopted instead to compute the discharge shown as:

$$Q = sign\{\lambda[h_m - h_d]cW\sqrt{2g}(h_U - z_{crest})(h_U - h_D)^{1/2}\} \tag{8}$$

If $h_U - z_{crest} \geq (A_0/W)$, the manhole is considered fully submerged and the orifice equation is used:

$$Q = sign\{\lambda[h_m - h_d]c_0 A_0\sqrt{2g}(h_U - h_D)^{1/2}\} \tag{9}$$

where c_0 is the orifice discharge coefficient.

Evaluation of model performance

In this study, three metrics are utilized to assess the model performance, including the Fit statistic (F), relative error (RE), and Root-Mean-Square Error ($RMSE$). Both the F statistic and $RMSE$ are commonly used for evaluating hydrodynamic models (Yin & Yu 2016). The F statistic is defined as follows:

$$F = \frac{A_{sim}}{A_{obs} + A_{sim} - A_0} \tag{10}$$

in which A_{obs} and A_{sim} indicate the sets of pixels observed to be flooded and predicted as flooded, respectively. A_0 is the overlap of A_{obs} and A_{sim}. F is equal to 1 when observed and predicted flooding areas coincide exactly, and 0 when no overlap exists. RE can be inferred based on the following equation:

$$RE = \frac{h_{\max}^{sim} - h_{\max}^{obs}}{h_{\max}^{obs}} \times 100\% \tag{11}$$

in which $h_{\max}^{sim}$ and $h_{\max}^{obs}$ denote predicted and observed maximum flooding depth. While the $RMSE$ metric is defined by:

$$RMSE = \left[\frac{1}{n} \sum_{i=1}^{n} (h_i^{sim} - h_i^{obs})^2\right]^{1/2} \tag{12}$$

where h_i^{sim} and h_i^{obs} represent predicted and observed flooding depths (or water levels), respectively; i is the index of wet pixels and n is the total number of wet pixels in prediction and observation.

APPLICATION

Case site

The coupled model was first tested on a real-world case study. The study concerns a watershed, i.e. the Shiqiao Creek District (SCD) in the downtown of Dongguan City, South China (Figure 2(a)–2(c)). This place is a nearly closed watershed and is one of the most severe flood-prone areas in Dongguan City (Wu *et al.* 2016), which is located along the Dongyin Canal and the Shiqiao Creek, with an approximate area of $2\,\text{km}^2$. Terrain elevations vary from 1.78 to 31.21 m and the climate regime belongs to the subtropical monsoon (Wu *et al.* 2017a, 2017b). The annual average rainfall and temperature are 1,770 mm and 22 °C, respectively. SCD is a highly urbanized area where urban land use accounts for over 80% of the total. The drainage system in SCD consists of the open Dongyin Canal, the closed Shiqiao Creek (covered by roads at present), as shown in Figure 2(c), and sewers. The sewers have been reinforced several times recently, yet some of the pipelines are still inadequate to drain surface storm water away, resulting in severe flooding problems.

Data

The DEM of SCD, with a high resolution of 1×1 m, was processed and quality controlled by the Urban Planning Bureau of Dongguan City (UPBDC). To reflect the blockage effect of buildings on surface flows, a Google satellite image of SCD was used to delineate the building profiles from the original DEM. For building height, note that there is no need to consider the actual height in the modeling, the elevation of the building zones in SCD was set to a fixed value of 10 m (Figure 2(d)).

Hourly rainfall data used in this case study were collected from a local rain gauge operated by the Meteorological Bureau of Dongguan City. The data set contains four extreme storm events, as listed in Table 1. There are no aerial images or instrument measurements of flood extent for these four events. However, point-based field surveys of flood locations and depths are available. The surveys mainly cover zones A, B, C and D (Figure 2), where instrument measurements of flooding depths were carried out by a crew from the Water Authority of Dongguan City. The crew are specialized in flood information collection and have visited the four zones mentioned above during the storm events (Wu *et al.* 2017a, 2017b). Therefore, the surveys, on the whole, can estimate a reasonable set of flooding depths over these zones. With the flooding depth data, the above-ground water levels across these zones were determined, based on elevations and flooding depths.
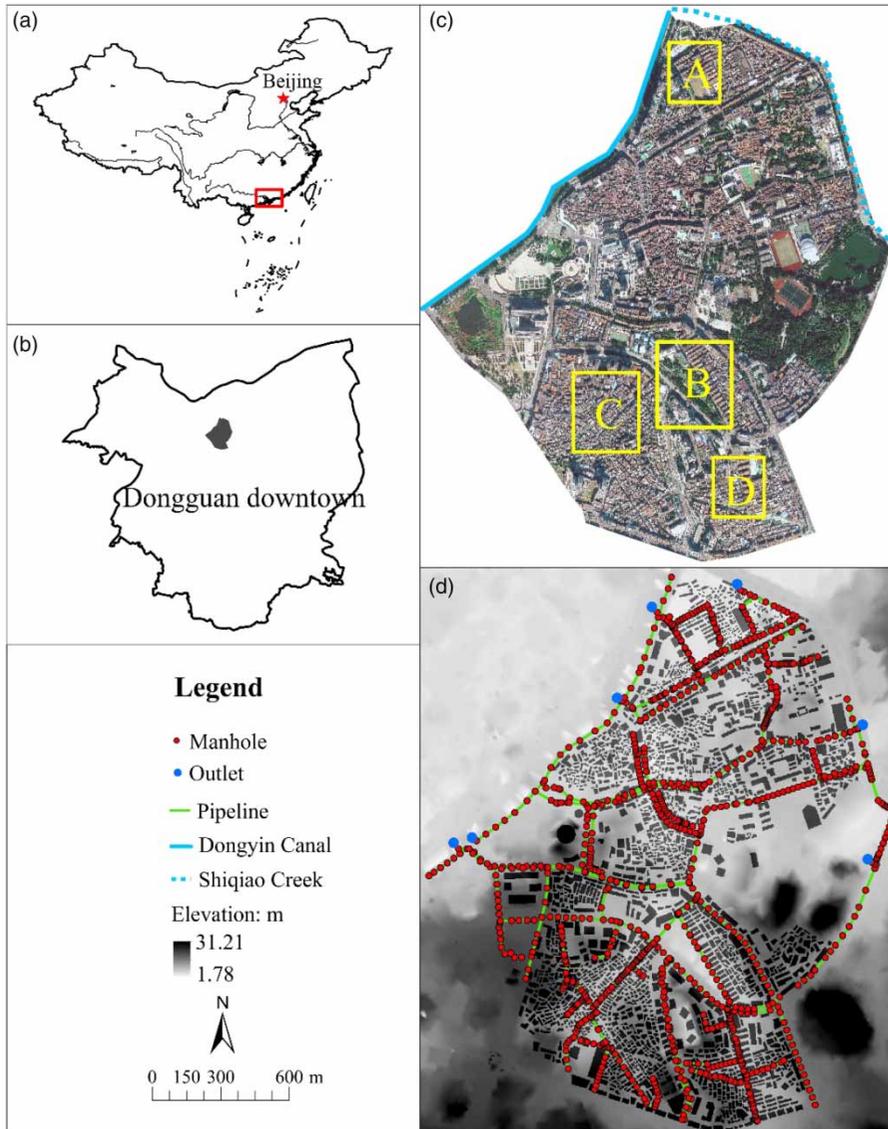
Figure 2 │ (a)–(c) Location of the case study region. Rectangles marked with 'A', 'B', 'C' and 'D' in (c) show severely flood-prone areas: **A**. Radio & TV University; **B**. Grass Pond; **C**. Jinniu Road; **D**. Aonan Road. (d) Top view of the DEM (with the building layer) of the study region with the sewer network and seven outlets.

Table 1 │ Four extreme storm events used in this study

Date	2005-08-20	2008-06-13	2014-03-30	2015-05-20
Rainfall amount/mm	184.3	351.6	197.8	204.1
Rainfall concentrated period	00:00–06:00	06:00–10:00	07:00–13:00	04:00–11:00

In other words, water levels in zones A, B, C and D are approximately equal to local elevations plus flooding depths (this process was done by means of GIS). Regions with water levels greater than zero were regarded as flooding and then the flooding extents over these regions were obtained (Table 2).

The drainage network data were obtained from UPBDC. Some of the pipelines and manholes were constructed

**Table 2** │ Four historical flooding events used in the study

Flooding date	Flooding site	Zone A	Zone B	Zone C	Zone D
2005-08-20	Maximum flooding depth/m	0.70	1.80	0.90	/
	Maximum flooding depth/m^2	8,000	31,000	26,000	/
2008-06-13	Maximum flooding depth/m	1.00	2.00	1.10	1.20
	Maximum flooding depth/m^2	10,000	33,000	27,000	12,000
2014-03-30	Maximum flooding depth/m	0.80	1.80	0.90	/
	Maximum flooding depth/m^2	8,500	31,000	26,000	/
2015-05-20	Maximum flooding depth/m	0.90	1.90	1.00	1.00
	Maximum flooding depth/m^2	9,000	32,500	26,500	10,000

around the 1940s, and are now blocked and should be neglected when modeling. Finally, the simplified sewer network contains seven outlets, 989 manholes and 990 pipelines (Figure 2(d)). In addition, this case study took the water level of Dongyin Canal as one of the boundary conditions (Figure 3), and the corresponding data were provided by the Disaster Prevention Headquarters of Dongguan City.

Testing results

Model setup

The SWMM time step in this study was set to a fixed value of 2s. In regard to the LISFLOOD-FP time step, an adaptive
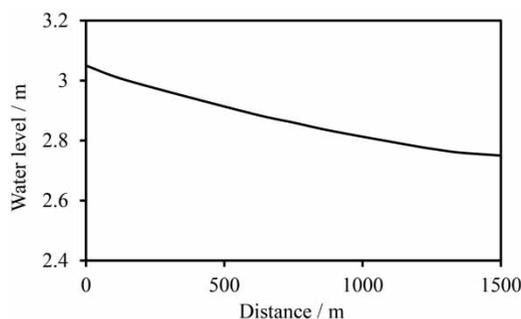
Figure 3 │ Water surface curve of the Dongyin Canal starting from upstream (the upper edge of SCD) to downstream (the left edge of SCD).

time step was used in order to avoid model instability (Bates *et al.* 2010). The total simulation time was 24 h covering the whole day. With respect to the boundary conditions, the Shiqiao Creek is closed and covered by roads at present and should be regarded as a sub-drain that belongs to the sewer network. Therefore, all boundaries except the fixed river level boundary (the Dongyin Canal) in the west side of the modeled area were free. Because base flow data of the sewers were unavailable in the application, the base flows in the pipelines were assumed to be zero before simulation. Given the fact that in rainy days evapotranspiration in a region is always weak due to the high humidity condition, the evapotranspiration in SCD during a storm event is negligible and was not considered in the modeling.

Calibration

The major parameters that play key roles in the coupled 1D/2D model and need to be calibrated consist of Manning's coefficients of the 2D overland surface, the 1D river channel and pipelines, and the soil infiltration rate (Bates *et al.* 2010; Leandro & Martins 2016). These parameters were calibrated based on two historical storm events that respectively occurred on August 19th, 2005 and on March 30th, 2014 in the study area. The three metrics, i.e. *RE*, *F* statistic, and *RMSE*, were used for goodness-of-fit measurements between the observed and simulated flooding. The reduction coefficient proposed in the current study is also a key parameter, however it is mainly determined by Equation (3) and should be kept constant during the calibration process. The other parameters, including the depression storage depth and the Horton infiltration parameters, because they usually show little influence on simulation results (Zhu *et al.* 2016), were not calibrated and the default values based on the SWMM operators were used. The calibrated ranges of the aforementioned key parameters and the other parameters with default values are presented in Table 3.

Figure 4 shows the simulated flooding for the two observed storm events. Note that the simulated severely flooding sites coincide with the flood-prone areas outlined in Figure 2. Table 4 further summarizes the predicted and observed maximum flooding depths and extents for two

Table 3 | Parameters used in the coupled 1D/2D model

| Parameter	Type	Calibrated values
Roughness value of 1D pipelines	Brick	0.012–0.018
	Cast iron	0.010–0.016
	Concrete	0.011–0.015
	PVC	0.010–0.013
Roughness of 1D river channel	/	0.020–0.040
Roughness of 2D overland surface	Road	0.011–0.015
	Building area	0.022–0.026
	Grassland	0.200–0.300
	Wasteland	0.040–0.080
	Shrub land	0.400–0.500
Depression storage depth	Permeable	5.0 mm[a]
	Impermeable	2.5 mm[a]
Horton infiltration parameters	Maximum rate	100 mm/h[a]
	Minimum rate	10 mm/h[a]
	Decay constant	9 h^{-1}[a]
	Drying time	7 d[a]
Discharge reduction coefficient of manhole	/	0.75

Note: [a]indicates default values from model operators.

events at the severe flooding sites. As the results show, the coupled model is capable of capturing the maximum flooding depths and extents in these regions, on the whole. The *RE* values of predicted extents for two calibrated events fall between −12.5% and 0, while those of the predicted extents range from −2.5 to −0.77%, with *F* values all greater than 0.8. In terms of *RMSE*, the values are between 0.7 and 0.26, which again indicates a reasonable model performance. For SCD as a whole, the *RE*, *F* and *RMSE* metrics are within the acceptable ranges. Figure 5 depicts the water balance (mass balance) components over the model domain for two calibration events. It is shown that the input water volume, i.e. rainfall, is approximately equal to the sum of outflow and flooding volumes. Overall, the coupled 1D/2D model is considered to perform well for two calibration flooding events, which further suggests that the calibrated values of model parameters in Table 3 are reasonable and suitable for the subsequent model validation.
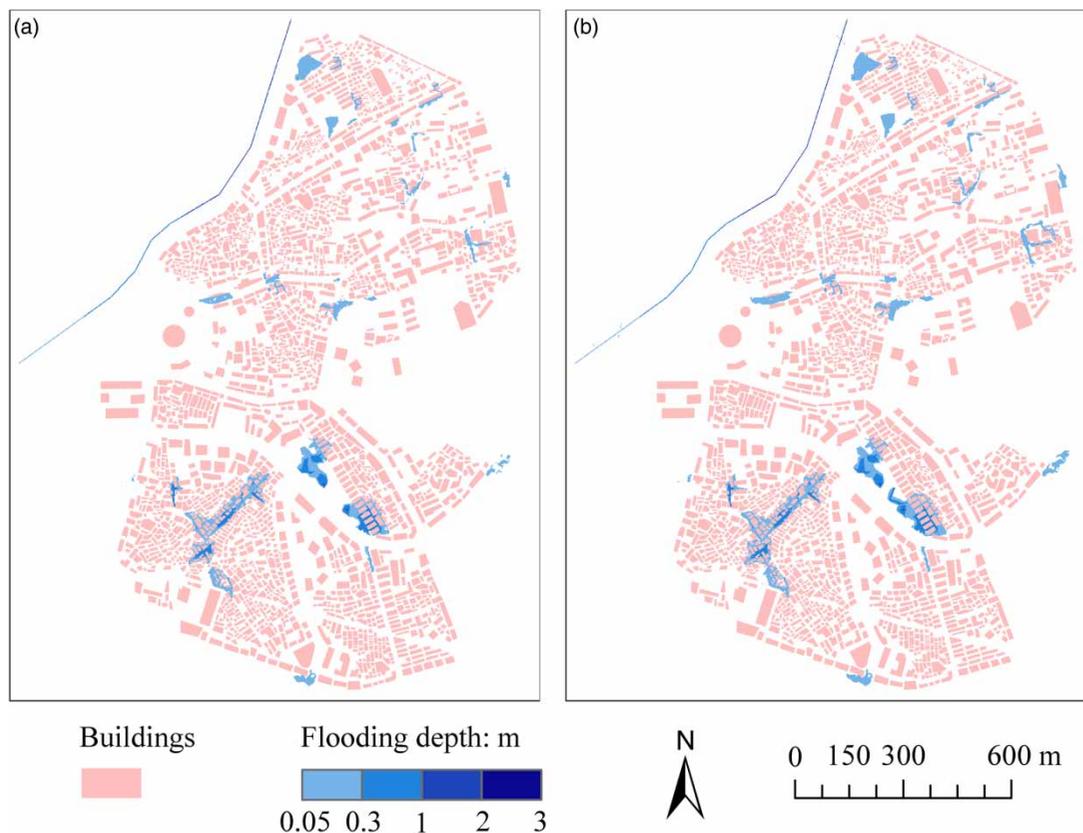
Figure 4 | Maximum flooding depth maps of the (a) August 20th, 2005 and (b) March 30th, 2014 flood events predicted by the coupled 1D/2D hydrodynamic model.

Table 4 | Calibration results of the coupled 1D/2D model

Flooding site	Flooding date	Maximum flooding depth			Maximum flooding extent			F statistic	RMSE
		Record	Simulated	RE	Record	Simulated	RE		
Zone A	2005-08-20	0.70 m	0.65 m	−7.14%	8,000 m^2	7,800 m^2	−2.50%	0.84	0.19
	2014-03-30	0.80 m	0.70 m	−12.50%	8,500 m^2	8,300 m^2	−2.35%	0.86	0.17
Zone B	2005-08-20	1.80 m	1.75 m	−2.78%	31,000 m^2	30,600 m^2	−1.29%	0.87	0.17
	2014-03-30	1.80 m	1.70 m	−5.56%	31,000 m^2	30,300 m^2	−2.26%	0.85	0.20
Zone C	2005-08-20	0.90 m	0.90 m	0.00%	26,000 m^2	25,700 m^2	−1.15%	0.82	0.23
	2014-03-30	0.90 m	0.85 m	−5.56%	26,000 m^2	25,800 m^2	−0.77%	0.81	0.26
Whole region	2005-08-20	1.80 m	1.75 m	−2.78%	82,000 m^2	79,500 m^2	−3.05%	0.75	0.30
	2014-03-30	1.80 m	1.70 m	−5.56%	84,000 m^2	81,000 m^2	−3.57%	0.73	0.32
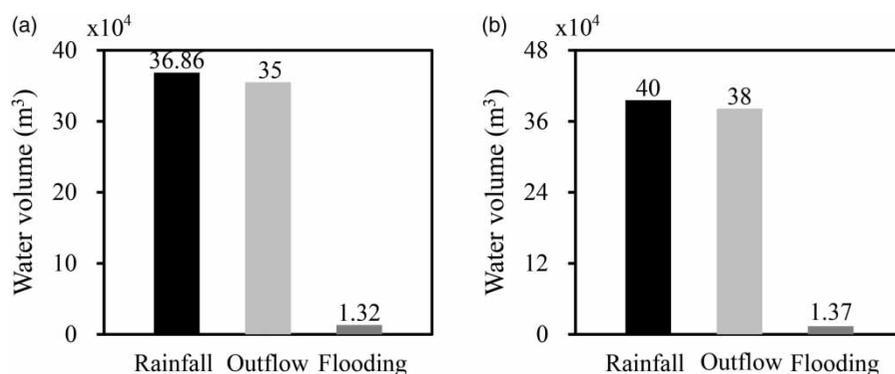
Figure 5 | Modeled water balance for the (a) August 20th, 2005 and (b) March 30th, 2014 flood events over the SCD domain at the end of the simulations.

Validation

After the calibration process, the coupled model was validated against another two historical flood events that respectively struck SCD on June 13th, 2008 and on May 20th, 2015. Results indicate that Zones A, B, C and D are the most severe flooding areas across SCD (Figure 6). For the two flood events, the simulated maximum flooding depths and extents at these sites are in accord with the records on the whole (Table 5). When looking more closely at the results, the relative errors of the depths vary from −16.67 to −5%, and those of the extents are between −6.67 and −0.75%. At the same time, the F statistics for these regions are generally greater than 0.8, with RMSE values within the range of 0.23–0.31. In regard to water balance, as Figure 7 indicates, no significant differences are seen in the water balance errors. These results altogether can provide confidence in model capability in predicting urban flooding.

DISCUSSION

Computational cost

Although simplified 2D models or coupled 1D/2D models have advantages of simulating 2D floodplain flows, computational cost, which is due to the need to adopt very small time steps to avoid numerical instabilities in relation to small water depths and surface irregularities (Paz *et al.* 2016), has become a main drawback of these models. Such a drawback would become more apparent when high-quality data are used (Dottori *et al.* 2013; Bach *et al.* 2014). This specific case study used detailed data sets, including rainfall data of four historical 24-h storm events, a high spatial resolution (1 × 1 m) DEM, and a complex sewer network (even has been simplified before simulation) consisting of approximately 1,000 manholes and pipelines. The application also employed a 2-s time step of SWMM along with an adaptive
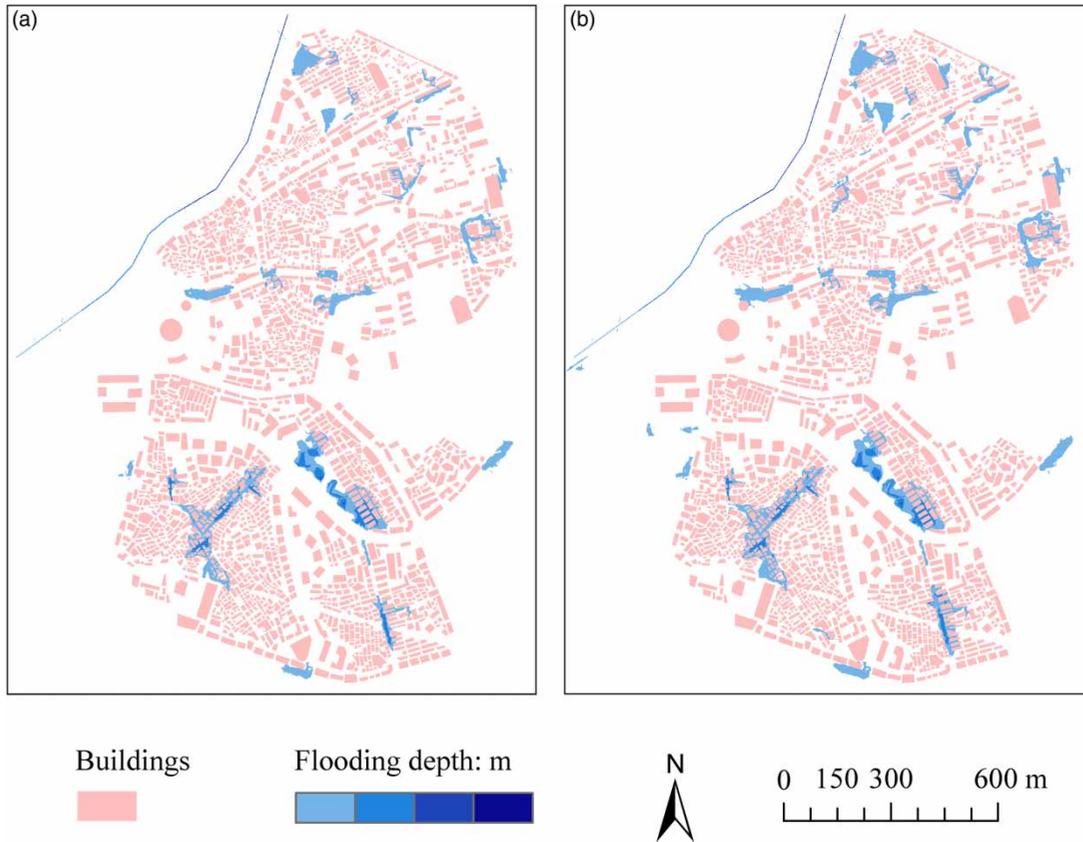
Figure 6 │ Maximum flooding depth maps of the (a) June 13th, 2008 and (b) May 20th, 2015 flood events predicted by the coupled 1D/2D hydrodynamic model.

time step of LISFLOOD-FP, for the purpose of relatively accurate simulation. Accordingly, the model managed to run each simulation within 6 h in a 3.3 GHz Intel processor with 8 GB RAM. The 6-h runtime seems long in terms of flood prediction, but is within the acceptable range considering that detailed data sets were utilized and it is computationally demanding (Hunter et al. 2005; Dottori et al. 2013; Paz et al. 2016; Ming et al. 2017a 2017b).

Table 5 │ Validation results of the coupled 1D/2D model

Flooding site	Flooding date	Maximum flooding depth			Maximum flooding extent			F statistic	RMSE
		Record	Simulated	RE	Record	Simulated	RE		
Zone A	2008-06-13	1.00 m	0.85 m	−15.00%	10,000 m²	9,500 m²	−5.00%	0.82	0.24
	2015-05-20	0.90 m	0.75 m	−16.67%	9,000 m²	8,500 m²	−5.56%	0.81	0.24
Zone B	2008-06-13	2.00 m	1.85 m	−7.50%	33,000 m²	32,200 m²	−2.42%	0.83	0.23
	2015-05-20	1.90 m	1.80 m	−5.26%	32,50 ²	31,500 m²	−3.08%	0.82	0.26
Zone C	2008-06-13	1.10 m	1.00 m	−9.09%	27,000 m²	26,500 m²	−1.85%	0.80	0.27
	2015-05-20	1.00 m	0.95 m	−5.00%	26,500 m²	26,300 m²	−0.75%	0.78	0.31
Zone D	2008-06-13	1.20 m	1.00 m	−16.67%	12,000 m²	11,200 m²	−6.67%	0.85	0.22
	2015-05-20	1.00 m	0.90 m	−10.00%	10,000 m²	9,500 m²	−5.00%	0.85	0.22
Whole region	2008-06-13	2.00 m	1.85 m	−7.50%	120,000 m²	110,000 m²	−8.33%	0.71	0.37
	2015-05-20	1.90 m	1.80 m	−5.26%	95,000 m²	88,000 m²	−7.37%	0.70	0.38
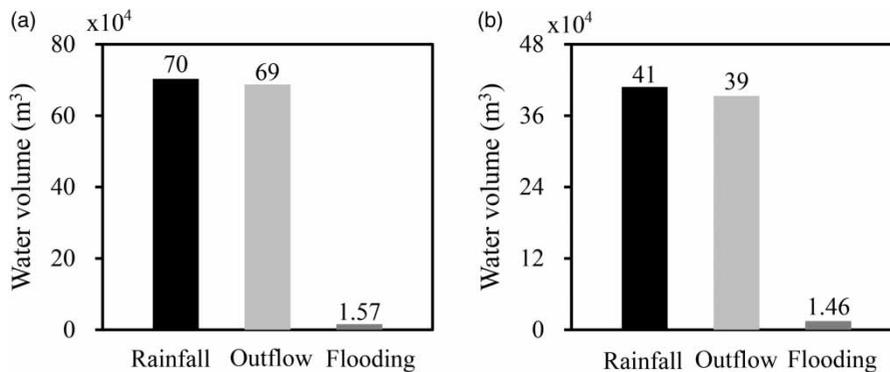
Figure 7 │ Modeled water balance for the (a) June 13th, 2008 and (b) May 20th, 2015 flood events over the SCD domain at the end of the simulations.

Effect of reduction coefficient on model performance

The interacting discharge between sewer and surface is influenced by multiple factors, such as the size and shape of the manhole, and debris-induced blocking. It is therefore impossible to precisely measure the real discharge capacity for a manhole. In the current research the effect of manhole shape on interacting discharge is preliminarily considered and reflected by the reduction coefficient involved in the pre-existing weir and orifice formulas. The model capability of capturing the surface flow routing dynamics in the application on one hand indicates the reasonability of coupling SWMM and LISFLOOD-FP, and to some extent supports the use of such a reduction coefficient on the other.

To further assess how the reduction coefficient affects model parameter specifications and simulated results, the coupled 1D/2D model was additionally operated without considering the reduction coefficient to simulate the four historical flood events. Correspondingly, the model parameters listed in Table 3 were recalibrated against the August 19th, 2005 and March 30th, 2014 floods. The recalibrated parameter values and the simulation results were then compared to those presented earlier. It is found that the 2D surface roughness is sensitive to the reduction coefficient while other parameters

are less so. As Table 6 illustrates, the upper ranges of roughness will generally increase if the reduction coefficient is not involved in simulation. The means of roughness values are larger than those with the reduction coefficient considered in the modeling. In particular, the mean roughness of building areas would increase approximately 50%. Table 7 compares the modeled results of four flood-prone areas before and after the reduction coefficient was applied to the coupled model. It is also clear that the model accuracy will decrease if the reduction coefficient is not considered. All these findings indicate that the 1D/2D model with reduction coefficient applied somewhat outperforms that without the reduction coefficient. Therefore, the effect of manhole-cover on manhole discharge capacity is indeed an important factor which may cause divergence of model parameter specifications and affect model accuracy. However, given that it is the first attempt to discuss the manhole-cover effect, the reduction coefficient and its estimation formula acquires stepwise demonstration or improvement in future work.

Advantages and caveats of the coupled 1D/2D model

The coupled 1D/2D model proposed here can be readily integrated with GIS because its output file format is

Table 6 │ Comparison of 2D overland roughness values before and after the reduction coefficient was applied to the model

Surface type		Road	Building area	Grassland	Wasteland	Shrub land
Reduction coefficient applied	Range	0.011–0.015	0.022–0.026	0.200–0.300	0.040–0.080	0.400–0.500
	Mean	0.013	0.0240	0.250	0.060	0.450
No reduction coefficient	Range	0.010–0.020	0.030–0.040	0.250–0.300	0.060–0.100	0.350–0.550
	Mean	0.015	0.035	0.270	0.080	0.440

Table 7 | Comparison of modeled results before and after the reduction coefficient was applied to the model

Flooding date	Flooding site	Maximum flooding depth/m				Maximum flooding extent/m²			
		Zone A	Zone B	Zone C	Zone D	Zone A	Zone B	Zone C	Zone D
2005-08-20	Record	0.70	1.80	0.90	/	8,000	31,000	26,000	/
	Y	0.65	1.75	0.90	/	7,800	30,600	25,700	/
	N	0.60	1.65	0.80	/	7,500	30,000	25,600	/
2008-06-13	Record	1.00	2.00	1.10	1.20	10,000	33,000	27,000	12,000
	Y	0.85	1.85	1.00	1.00	9,500	32,200	26,500	11,200
	N	1.00	1.70	0.90	0.90	9,000	31,500	26,500	10,800
2014-03-30	Record	0.80	1.80	0.90	/	8,500	31,000	26,000	/
	Y	0.70	1.70	0.85	/	8,300	30,300	25,800	/
	N	0.65	1.60	0.90	/	7,800	30,000	25,500	/
2015-05-20	Record	0.90	1.90	1.00	1.00	9,000	32,500	26,500	10,000
	Y	0.75	1.80	0.95	0.90	8,500	31,500	26,300	9,500
	N	0.70	1.65	0.85	0.75	8,500	30,700	25,800	9,000

Note: Y denotes reduction coefficient used, and N indicates no reduction coefficient used.

raster-based (Bates & De Roo 2000), and such a feature is considered convenient for model post-processing and is something that many existing coupled 1D/2D models do not have. Another potential advantage is that it does not employ commercial modules which means that it can possibly be used by all users. Also, the simple structures of SWMM and LISFLOOD-FP allow the coupled model to be set up easily, and therefore suitable for non-expert users.

It is worth mentioning that although the coupled 1D/2D model is verified to make a reasonable fit to the observed flood events, the model accuracy is almost invariably affected by various uncertainty sources derived from assumptions of modeling conditions, parameter specification and data quality (Wang *et al.* 2014), which have not been quantitatively investigated in this research. Therefore, substantially more validation should be carried out to further verify the model and caution should be taken when applying it to other scenarios (Ming *et al.* 2017a, 2017b).

CONCLUSION

This paper has sought to introduce a simplified approach for predicting urban flooding by means of coupling SWMM and LISFLOOD-FP. In the coupled model framework, SWMM is used to simulate dynamic flows in 1D sewers, while LISFLOOD-FP deals with 1D river channel flows and 2D overland flow propagation. Meanwhile, the model is able to reproduce the interaction between the sewer flow and the surcharge-induced flooding.

The real-life application results demonstrate the ability of the coupled 1D/2D model in dealing with urban flooding problems. While the successful coupling of SWMM and LISFLOOD-FP provides another approach for predicting urban flood, further studies should be done in the future, working around the model uncertainty, improvement of computational efficiency, and integration with GIS.

ACKNOWLEDGEMENTS

REFERENCES

Apel, H., Aronica, G. T., Kreibich, H. & Thieken, A. H. 2009 Flood risk analyses – how detailed do we need to be? *Nat. Hazards* **49**, 79–98.

Bach, P. M., Rauch, W., Mikkelsen, P. S., McCarthy, D. T. & Deletic, A. 2014 A critical review of integrated urban water modelling – urban drainage and beyond. *Environ. Modell. Software* **54**, 88–107.

Bates, P. D. & De Roo, A. P. J. 2000 A simple raster-based model for flood inundation simulation. *J. Hydrol.* **236**, 54–77.

Bates, P. D., Horritt, M. S. & Fewtrell, T. J. 2010 A simple inertial formulation of the shallow water equations for efficient two-dimensional flood inundation modelling. *J. Hydrol.* **387**, 33–45.

Chang, T. J., Wang, C. H. & Chen, A. S. 2015 A novel approach to model dynamic flow interactions between storm sewer system and overland surface for different land covers in urban areas. *J. Hydrol.* **524**, 662–679.

de Almeida, G. A. M., Bates, P. D., Freer, J. & Souvignet, M. 2012 Improving the stability of a simple formulation of the shallow water equations for 2-D flood modeling. *Water Resour. Res.* **48**, W05528. doi: 10.1029/2011WR011570.

Delleur, J. W. 2003 The evolution of urban hydrology: past, present, and future. *J. Hydraul. Eng.* **129**, 563–573.

Dottori, F., Di Baldassarre, G. & Todini, E. 2013 Detailed data is welcome, but with a pinch of salt: accuracy, precision, and uncertainty in flood inundation modeling. *Water Resour. Res.* **49**, 6079–6085.

Her, Y. & Chaubey, I. 2015 Impact of the numbers of observations and calibration parameters on equifinality, model performance, and output and parameter uncertainty. *Hydrol. Process.* **29**, 4220–4237.

Hunter, N. M., Horritt, M. S., Bates, P. D., Wilson, M. D. & Werner, M. G. F. 2005 An adaptive time step solution for raster-based storage cell modelling of floodplain inundation. *Adv. Water Resour.* **28**, 975–991.

Kjeldsen, T. R., Miller, J. D. & Packman, J. C. 2013 Modelling design flood hydrographs in catchments with mixed urban and rural land cover. *Hydrol. Res.* **44**, 1040–1057.

Leandro, J. & Martins, R. 2016 A methodology for linking 2D overland flow models with the sewer network model SWMM 5.1 based on dynamic link libraries. *Water Sci. Technol.* **73**, 3017–3026. doi: 10.2166/wst. 2016.171.

Leandro, J., Chen, A. S., Djordjević, S. & Savić, D. A. 2009 Comparison of 1D/1D and 1D/2D coupled (Sewer/Surface) hydraulic models for urban flood simulation. *J. Hydraul. Eng.* **135**, 495–504.

Leandro, J., Schumann, A. & Pfister, A. 2016 A step towards considering the spatial heterogeneity of urban key features in urban hydrology flood modelling. *J. Hydrol.* **535**, 356–365.

Leitão, J. P., do Céu Almeida, M., Simões, N. E. & Martins, A. 2013 Methodology for qualitative urban flooding risk assessment. *Water Sci. Technol.* **68**, 829–838.

Liang, Q. & Smith, L. 2015 A high-performance integrated hydrodynamic modelling system for urban flood simulation. *J. Hydroinform.* **17**, 518–533.

Lin, K., Lv, F., Chen, L., Singh, V. P., Zhang, Q. & Chen, X. 2014 Xinanjiang model combined with Curve Number to simulate the effect of land use change on environmental flow. *J. Hydrol.* **519**, 3142–3315.

Ming, B., Liu, P., Bai, T., Tang, R. & Feng, M. 2017a Improving optimization efficiency for reservoir operation using a search space reduction method. *Water Resour. Manag.* **31** (4), 1173–1190. doi: 10.1007/s11269-017-1569-x.

Ming, B., Liu, P., Guo, S., Zhang, X., Feng, M. & Wang, X. 2017b Optimizing utility-scale photovoltaic power generation for integration into a hydropower reservoir by incorporating long- and short-term operational decisions. *Appl. Energy* **204**, 432–445.

Paz, A. R., Serra, L. S., de Freitas Silva, M. R. & Meller, A. 2016 Reducing computational runtime of two-dimensional urban inundation model by dynamic domain reshaping. *J. Hydrol. Eng.* **21**, 04016013.

Salarpour, M., Rahman, N. A. & Yusop, Z. 2011 Simulation of flood extent mapping by InfoWorks RS-case study for tropical catchment. *J. Softw. Eng.* **5**, 127–135.

Seyoum, S. D., Vojinovic, Z., Price, R. K. & Weesakul, S. 2012 Coupled 1D and noninertia 2D flood inundation model for simulation of urban flooding. *J. Hydraul. Eng.* **138**, 23–34.

Swan, A. 2010 How increased urbanisation has induced flooding problems in the UK: a lesson for African cities? *Phys. Chem. Earth* **35**, 643–647.

Wang, W., Yu, Z., Zhang, W. & Shao, Q. 2014 Responses of rice yield, irrigation water requirement and water use efficiency to climate change in China: historical simulation and future projections. *Agr. Water Manage.* **146**, 249–261.

Willems, P., Arnbjerg-Nielsen, K., Olsson, J. & Nguyen, V. T. V. 2012 Climate change impact assessment on urban rainfall extremes and urban drainage: methods and shortcomings. *Atmos. Res.* **103**, 106–118.

Wu, X., Wang, Z., Zhou, X., Lai, C., Lin, W. & Chen, X. 2016 Observed changes in precipitation extremes across 11 basins in China during 1961–2013. *Int. J. Climatol.* **36**, 2866–2885.

Wu, X., Wang, Z., Guo, S., Liao, W., Zeng, Z. & Chen, X. 2017a Scenario-based projections of future urban inundation within a coupled hydrodynamic model framework: a case study in Dongguan City, China. *J. Hydrol.* **547**, 428–442.

Wu, X., Wang, Z., Zhou, X., Lai, C. & Chen, X. 2017b Trends in temperature extremes over nine integrated agricultural regions in China, 1961–2011. *Theor. Appl. Climatol.* **129**, 1279–1294. doi: 10.1007/s00704-016-1848-0.

XP Software 2013 *Technical Description XP Solution*.

Yin, J. & Yu, D. 2016 Coupled modeling of storm surge and coastal inundation: a case study in New York City during Hurricane Sandy. *Water Resour. Res.* **52**. doi: 10.1002/2016WR019102.

Zhu, Z., Chen, Z., Chen, X. & He, P. 2016 Approach for evaluating inundation risks in urban drainage systems. *Sci. Total. Environ.* **553**, 1–12.